CHIN. PHYS. LETT. Vol. 35, No. 5 (2018) 058401

A Simpler Memristor Emulator Based on Varactor Diode

Dong-Sheng Yu(于东升)[1], Ting-Ting Sun(孙婷婷)[1], Ci-Yan Zheng(郑辞晏)[2], H. H. C. Iu[2], T. Fernando[2]**

[1]*School of Electrical and Power Engineering, China University of Mining and Technology, Xuzhou 221116*

[2]*School of Electrical, Electronic and Computer Engineering, The University of Western Australia, Perth WA 6009, Australia*

(Received 12 January 2018)

A new memristor (MR) emulator is designed by making use of only three current-feedback operational amplifiers, one varactor diode, one capacitor and five resistors. As compared with other reported MR emulators, only three active devices and ten components in total are required for realizing this MR emulator, and hence this emulator can be regarded as a simpler one for the moment. The results obtained by Multisim simulation and experimental prototypes are given to verify the practicality and feasibility of this MR emulator.

PACS: 84.30.−r, 84.30.Bv, 85.25.Hv DOI: 10.1088/0256-307X/35/5/058401

As a unique two-terminal fundamental circuit element with information storage ability, the memristor (MR) has attracted immense worldwide interest since the researchers at HP labs announced the successful fabrication of nanoscale memristive devices.[1,2] Since then, many MR devices have been designed and manufactured. By inserting a thin $A1O_\delta$ barrier layer between the electrode and the tantalum oxide resistive switching layer, triple-layer ReRAM devices with improved resistive switching performance are demonstrated.[3] The analog switching in HfO_x-based resistive memory with a thermal enhanced layer is proposed[4] for improving the switching speed and data retention. The nanoscale MR has been used to structure a neuromorphic network with gradual and continuous weight change,[5] and based on which, an integrated neuromorphic network hardware system is built and trained online for grey-scale face classification. The experimental implementation of sparse coding algorithms in a bio-inspired approach using a 32×32 crossbar array of analog MRs is reported.[6]

However, since MRs are still not commercially popularized, currently, MR emulators are still necessarily required to uncover the dynamic characteristics of MR-based circuits.[7−12] Many MR emulators have been proposed by making use of active devices and passive circuit components. As discussed in Ref. [7], in addition to fourteen resistors and one capacitor, five operation amplifiers and one JFET transistor are used to structure a ground MR emulator. An analog MR emulator with cubic nonlinearity is designed[8] for establishing the third-order chaotic oscillator circuit, of which three operational amplifiers and two multipliers are used. The light-dependent resistor (LDR) is employed to implement the MR emulator[9] along with three operational amplifiers, two capacitors and nine resistors. However, this MR emulator has the drawback of low accuracy of input current. A hardware circuit for emulating floating MRs is presented[10] by using one 6-bit analog-to-digital converter and one 6-bit resistive digital-to-analog converter in addition to two operational amplifiers. In Ref. [11], an analog circuit which can practically emulate floating MRs is proposed by utilizing four current-feedback operational amplifiers (CFOA) and four capacitors, in addition to two diodes and four resistors. This MR emulator is then used for achieving frequency-to-voltage conversion. A practical MR emulator is newly proposed[12] for mimicking the nonlinear behaviors of the well-known current controlled MRs, of which five active devices are desired. An MR emulator capable of operating with a wide range of the excitation frequency from 16 Hz to 160 kHz is presented.[13] These MR emulators have provided a good reference route for probing the inherent behaviors of MR-based circuits.

With regard to MR, its abilities of processing and storing information without the requirement of a power source would open up new realms for future circuit investigations and applications. Currently, in addition to mimicking the inherent dynamic behaviors of MRs, MR emulators have also been used beforehand in many functional circuits for exploring the possible applications of MRs. As discussed in Ref. [11], the newly proposed floating MR emulator is used for converting an FM signal to an AM signal by exploiting the advantage of the frequency-dependence of the memristance. The MR emulators have been attempted to be used for generating chaotic signals.[8] In Ref. [14], the MR emulators are employed to structure the relaxation oscillators to obtain square waveforms with adjustable frequency and duty cycle. The MR emulator is used for the realization of synapse functionalities in neuromorphic circuits such as long term potentiation, long term depression and synaptic plasticity.[15] MR emulators are also adopted for structuring filters, programmable logic circuit, and so on. These research works also reflect the importance of designing MR emulators with good performance.

In this Letter, a new MR emulator with fewer components is proposed with the attractive advantages of simple structure, small volume and low price. The proposed MR emulator circuit is presented in Fig. 1, in which a varactor diode is used, as enclosed by the dotted frame. The varactor diode possesses variable

**Corresponding author. Email: Tyrone.Fernando@uwa.edu.au

© 2018 Chinese Physical Society and IOP Publishing Ltd

barrier capacitance, which can be timely tuned by the imposed reverse voltage.

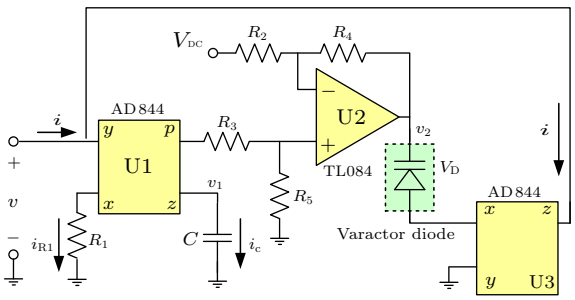

Fig. 1. The proposed MR emulator.

The variable capacitance of the varactor diode can be expressed as

$$C_{\rm vd} = C_{\rm vd0}\Big(\frac{V_{\rm bi}+v}{V_{\rm bi}}\Big)^{-\gamma}, \tag{1}$$

where $C_{\rm vd0}$ is the zero-bias diode capacitance, v denotes the reverse voltage, $V_{\rm bi}$ and γ are the built-in voltage and grading coefficient, respectively, and $C_{\rm vd0}$, $V_{\rm bi}$ and γ are determined by the physical fabrication of the varactor diode. Note that expression (1) could induce high complexities into the calculation of the equivalent MR constitutive relation. Hence, in comprehensive consideration of the calculation simplicity and accuracy, Eq. (1) can be fitted by the quadratic polynomial function and written as

$$C_{\rm vd} = a_0 + a_1 v + a_2 v^2, \tag{2}$$

where a_0, a_1 and a_2 are the fitting coefficients related to $C_{\rm vd0}$, $V_{\rm bi}$ and γ.

As shown in Fig. 1, only three active devices including two CFOAs (U1 and U3) and one operational amplifier (U2) are required. U1 is used for structuring the integral circuit to obtain equivalent flux ϕ. U2 and the resistors R_2, R_3, R_4, and R_5 are together establishing the differential subtraction circuit to ensure that the varactor operates under a reverse bias voltage. According to the operation performance of CFOA U1, the current outflowing terminal z is equal to the current going through resistor R_1. We have

$$i_{\rm c} = C\frac{dv_1}{dt} = i_{R1} = \frac{v}{R_1}. \tag{3}$$

Hence, the equivalent flux ϕ can be expressed as

$$\phi = \int v dt = R_1 C v_1. \tag{4}$$

Due to the function of the subtraction circuit, the output voltage of v_2 can be expressed as

$$v_2 = \alpha v_1 - \beta V_{\rm DC} = \frac{\alpha}{R_1 C}\phi - \beta V_{\rm DC}, \tag{5}$$

where

$$\alpha = \frac{R_2R_5 + R_5R_4}{R_2R_3 + R_2R_5},\ \beta = \frac{R_4}{R_2}.$$

Since there is no current going into terminal y of U1, and the charge going into terminal z of U2 is equal to the charge inputting terminal x of U2, we have

$$q = C_{\rm vd} v_2 = (a_0 + a_1 v_2 + a_2 v_2^2) v_2. \tag{6}$$

Substituting Eq. (5) into Eq. (6), we can obtain

$$q = \sigma + \zeta\phi + \kappa\phi^2 + \lambda\phi^3, \tag{7}$$

where

$$\begin{aligned}
\sigma &= -a_0\beta V_{\rm DC} + a_1\beta^2 V_{\rm DC}^2 - a_2\beta^3 V_{\rm DC}^3,\\
\kappa &= \frac{a_1\alpha^2 - 3a_2\alpha^2\beta V_{\rm DC}}{R_1^2C^2},\\
\zeta &= \frac{\alpha}{R_1C}(a_0 - 2a_1\beta V_{\rm DC} + 3a_2\beta^2 V_{\rm DC}^2),\\
\lambda &= \frac{a_2\alpha^3}{R_1^3C^3}.
\end{aligned}$$

Hence, the MR memductance can be obtained by conducting a derivation operation on both sides of Eq. (7)

$$W(\phi) = \frac{dq(\phi)}{d\phi} = 3\lambda\phi^2 + 2\kappa\phi + \zeta, \tag{8}$$

which reflects that the MR memductance can be timely varied by the equivalent flux ϕ. The value of ζ is equal to the initial memductance and can be adjusted by changing $V_{\rm DC}$.

The most attractive advantage of this newly proposed MR emulator is the requirement of fewer components. To comparatively display this advantage, the component numbers of the proposed and other reported MR emulators are listed in Table 1.

Table 1. Comparison of emulator component numbers.

Objectives		Component numbers for MR emulation							
		Ref. [7]	Ref. [8]	Ref. [9]	Ref. [10]	Ref. [11]	Ref. [12]	Ref. [13]	Proposed emulator
Op amps		5	3	3	2	0	2	0	1
CFOAs		0	0	0	0	4	2	2	2
Multipliers		0	2	0	0	0	1	1	0
Capacitors		1	1	1	1	4	1	3	1
Resistors		14	6	9	3	4	5	4	5
Diodes		0	0	1	4	2	0	0	1
Others	Active	0	0	0	3	0	0	1	0
	Passive	1	0	1	0	0	2	0	0
Total		21	12	15	13	14	13	11	10

It can be seen that, among the emulators listed in Table 1, the newly proposed emulator requires only ten components in total. The cells in the rows marked by Op amps, CFOAs, Multipliers and Active are filled by the number of active devices used for MR emulation. Evidently, only three active devices are required by the MR emulator shown in Fig. 1.

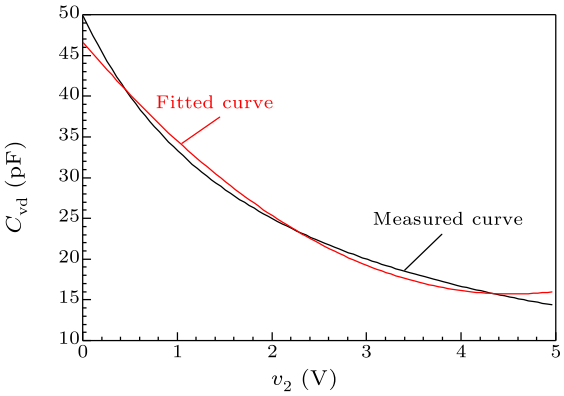

Fig. 2. The measured and fitted capacitance curve.

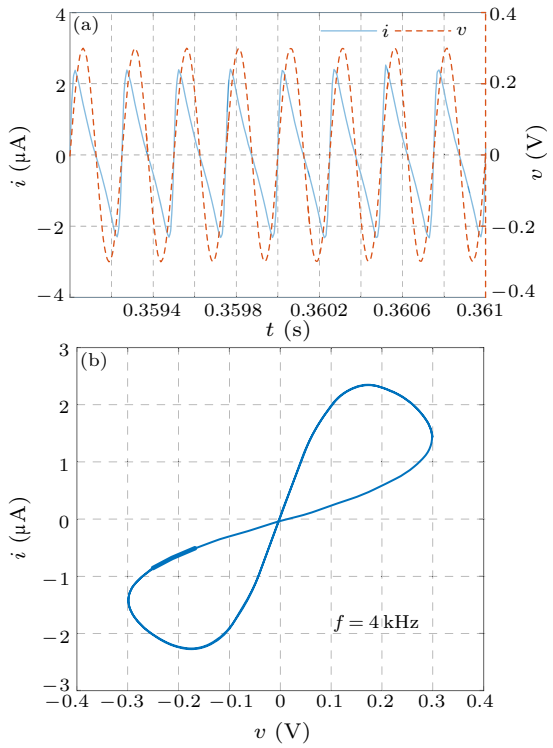

Fig. 3. Curves of the simulation results. (a) The simulation waveforms of v and i. (b) The simulation curves of the PHL.

The varactor diode used for structuring the MR emulator is BB910 manufactured by Shenzhen SI Semiconductors Co., LTD. The black curve drawn in Fig. 2 is reconstructed based on the capacitance data provided by the Shenzhen SI Semiconductors Co., LTD. The red curve is fitted based on the measured data by using quadratic polynomial. The fitting coefficients can be calculated as $a_0 = 0.4666e^{-10}$, $a_1 = -0.1366e^{-10}$ and $a_2 = 0.0151e^{-10}$. Note that, higher fitting accuracy can be obtained by using higher order polynomial if necessary.

The MR emulator is firstly established by Multisim and the circuit parameters are configured as $R_1 = 150\,\Omega$, $R_2 = R_3 = R_4 = R_5 = 75\,\text{k}\Omega$, $C = 12\,\text{nF}$, and $V_{\text{DC}} = -2.5\,\text{V}$. A sinusoidal voltage of $v = 0.3\sin(2\pi ft)$ in units of V with frequency $f = 4\,\text{kHz}$ is employed to test the MR emulator. The simulation results displayed in Fig. 3 reveal that the current passes through the origin together with the excitation voltage, and the pinched hysteresis loop (PHL) of excitation voltage v and the input current i is behaving as an inclined 8. These observed behaviors are in good agreement with typical MR characteristics.

To confirm the practical validation, the proposed emulator is built in hardware and then connected with a resistor of $10\,\text{k}\Omega$ in serial for testing, as shown in Fig. 4. Since the voltage v_{R} across resistor R is in proportion to the current going through MR, v_{R} is sampled for describing MR current i. By configuring the input voltage as $v_{\text{in}} = 0.3\sin(2\pi ft)$ in units of V with $f = 4\,\text{kHz}$, the sampled MR voltage v and equivalent current v_{R} in time domain are shown in Fig. 5(a), which displays high similarity with Fig. 3(a). The PHLs structured by v and v_{R} as frequency f equalling 4 kHz, 6 kHz and 9 kHz are presented in Figs. 5(b)–5(d), respectively. It can be seen that the PHLs are passing through the origin and evidently shrunk as the frequency f is increased, which is in good agreement with the typical feature of the MR called the frequency dependence of PHLs.

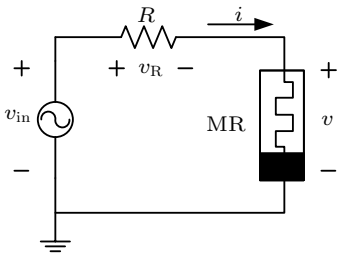

Fig. 4. The experimental test circuit.

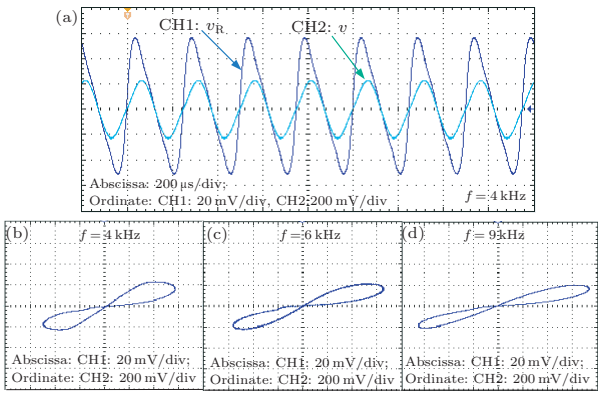

Fig. 5. The measured curves under sinusoidal excitation.

For the purpose of comprehensively testing, a

triangle-shaped voltage with 0.3 V amplitude and 4 kHz frequency is then adopted for exciting the circuit shown in Fig. 4. The measured MR voltage v and current i ($v_{\rm R}$ instead) in the time domain are presented in Fig. 6(a). Note that, although the measured current waveform shows an irregular shape, it is passing through the origin together with voltage v in stable periodicity. The Lissajous trajectory of v versus $v_{\rm R}$ is sampled and redrawn in Fig. 6(b) with the blue colour. This PHL looks like two fan blades with sharp ends. These experimental results reflect that the proposed emulator could provide good performance under different excitation conditions.

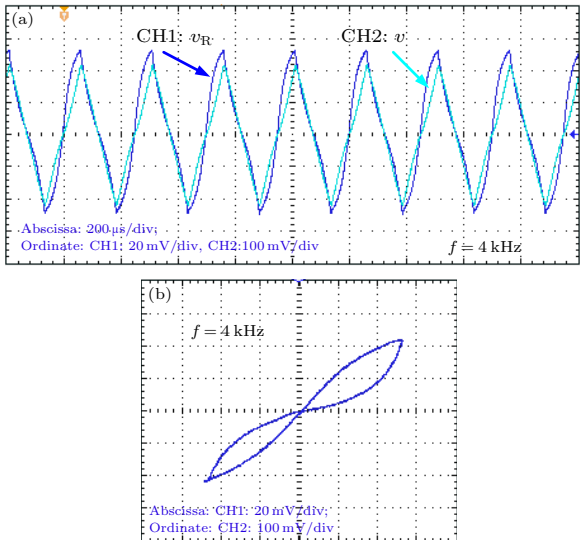

Fig. 6. The measured curves under triangular excitation.

The experimental results confirm that the proposed emulator with fewer components is capable of being practically applied, which is of great significance for designing or investigating emulator-based circuits, with the advantages of simple structure, small volume and low price.

In conclusion, making use of the controllable capacitance of the varactor diode, we propose a new MR emulator with fewer components, of which only three CFOAs, one capacitor and five resistors are required. The requirement of fewer components endows this MR emulator with the attractive advantages of smaller volume and lower price as compared with common emulators.

References

[1] Chua L O 1971 *IEEE Trans. Circuit Theory* **18** 507
[2] Strukov D B, Snider G S, Stewart D R et al 2008 *Nature* **453** 80
[3] Wu H Q, Li X Y, Wu M H et al 2014 *IEEE Electron Device Lett.* **35** 39
[4] Wu W, Wu H Q, Gao B et al 2017 *IEEE Electron Device Lett.* **38** 1019
[5] Yao P, Wu H Q, Gao B et al 2017 *Nat. Commun.* **8** 15199
[6] Sheridan P M, Cai F X, Du C et al 2017 *Nat. Nanotechnol.* **12** 784
[7] Valsa J, Biolek D and Biolek Z 2011 *Int. J. Numer. Model.* **24** 400
[8] Muthuswamy B 2010 *Int. J. Bifurcation Chaos Appl. Sci. Eng.* **20** 1335
[9] Fitch A L, Iu H H C, Wang X Y et al 2012 *IEEE Int Symp. Circuit Syst.(ISCAS)* (Seoul, South Korea) p 1139
[10] Shin S, Zheng L, Weickhardt G et al 2013 *IEEE Circuits Syst. Mag.* **13** 2
[11] Abuelma'Atti M T and Khalifa Z J 2016 *Analog Integr. Circuit Syst. Process.* **86** 141
[12] Alharbi A G, Fouda M E and Khalifa Z J et al 2017 *IEEE Access* **5** 5399
[13] Sánchez-López C, Carrasco-Aguilar M A and Muñiz-Montero C 2015 *Int. J. Electron. Commun.* **69** 1208
[14] Yu D S, Iu, H H C, Fitch A L et al 2014 *IEEE Trans. Circuit Syst. I-Regular Papers* **61** 2888
[15] Ranjan R, Ponce P M, Hellweg W L et al 2017 *J. Circuits Syst. Comput.* **26** 1750183